JOURNAL OF GUIDANCE, CONTROL, AND DYNAMICS
Vol. 30, No. 2, March–April 2007

Probabilistic Human Pilot Approach: Application to Microburst Escape Maneuver

Atilla Dogan* and Komkrit Kaewchay†
University of Texas at Arlington, Arlington, Texas 76019

DOI: 10.2514/1.25440

A new probabilistic approach is developed to study the effect of a group of pilots with a range of skill, training, and experience. Our probabilistic approach is based on the conception that there exists a set of parameters in a single pilot model that characterizes different aspects of human pilot behavior and reaction, and each of these characteristic parameters has a stochastic variation in a group of pilots. Thus, a group of pilots can be modeled by treating the characteristic parameters as random variables that follow suitable probability density functions. The probabilistic pilot model in combination with the Monte Carlo simulation technique is applied to study the sensitivity of three different microburst escape guidance strategies to human factors. In our study, both the human parameters as well as the microburst parameters are varied based on the probability density functions available in the literature and the intuition of the authors.

Nomenclature

$C_{\mathcal{M}_{(\cdot)}}$	=	pitching moment coefficient with respect to $(\cdot)$, N · m
$\bar{c}$	=	chord length, m
D	=	diameter of the peak radial outflow-velocity contour, m
D_K	=	set in which parameter vector $\underline{K}$ assumes values
D_θ	=	set in which parameter vector $\underline{\theta}$ assumes values
$E[\cdot]$	=	expected value of random variable $[\cdot]$
$F_{h_{\min}}(h)$	=	cumulative distribution function of $h_{\min}$
f_{f_h}	=	marginal probability density function of f_h
f_{f_r}	=	marginal probability density function of f_r
f_h	=	intensity of the downdraft, 1/s
f_r	=	intensity of the horizontal shear, 1/s
$f_{\theta K}$	=	joint probability density function of microburst and pilot parameters
h	=	altitude, m
h_c	=	commanded altitude, m
$h_{\min}$	=	minimum altitude reached in an escape maneuver, m
$I(\underline{\theta}, \underline{K}, h)$	=	minimum altitude indicator function
$I_{(\cdot)(\cdot)}$	=	moment or product of inertia, kg · m^2
$\underline{K}$	=	random pilot parameters vector
$\mathcal{L}$	=	rolling moment, N · m
$\mathcal{M}$	=	pitching moment, N · m
$\mathcal{N}$	=	yawing moment, N · m
n_m	=	variance of motor noise, rad^2
n_{oa}	=	variance of altitude observation noise, m^2
n_{ot}	=	variance of pitch angle observation noise, rad^2
p, q, r	=	components of angular velocity around body (x, y, z) axis, respectively, rad/s
$\mathcal{S}$	=	reference wing area, m^2
s	=	Laplace variable
T	=	thrust, N
V	=	airspeed, m/s
W_h	=	vertical wind velocity component, m/s
W_r	=	radial (horizontal) wind velocity component, m/s
W_x	=	horizontal wind velocity component in x direction, m/s
W_y	=	vertical wind velocity component in y direction, m/s
x	=	longitudinal distance from the runway threshold, m
x_c	=	location of microburst center in x direction, m
y	=	lateral distance from the runway threshold, m
y_c	=	location of microburst center in y direction, m
$\underline{z}_0$	=	initial condition of aircraft state vector

Subscript

rel	=	relative to air

Symbols

α	=	angle of attack, rad
Δz	=	moment arm of thrust around body y axis, m
$\Delta(\cdot)$	=	deviation of $(\cdot)$ from its commanded value
δ_e	=	elevator deflection, rad
θ	=	pitch angle, rad
$\underline{\theta}$	=	microburst parameters
θ_c	=	commanded pitch angle, rad
ρ	=	air density, kg/m^3
σ	=	parameter of Rayleigh probability distribution function
τ	=	time constant of reaction time delay model, s
τ_N	=	time constant of neuromuscular dynamics, s
ϕ	=	bank angle, rad
ψ_w	=	angle between the radial wind and x axis, rad

Presented as Paper 6031 at the AIAA Atmospheric Flight Mechanics Conference and Exhibit, San Francisco, California, 15–18 August 2005; received 25 May 2006; revision received 1 October 2006; accepted for publication 2 October 2006.

*Assistant Professor, Department of Mechanical and Aerospace Engineering. Senior Member AIAA.

†Graduate Student, Department of Mechanical and Aerospace Engineering.

I. Introduction

THE study of man–machine interfaces has been of great interest among researchers [1–5] for a considerable period of time. A specific, practical example involving such an interface is an aircraft flown by a human pilot [6–9]. The coupling between the human pilot and the airplane can lead to a variety of consequences ranging from pilot-induced oscillations [10,11] to even instability/stalling [12]. To study such interactions with the least danger and expense, many flight simulations [13,14] have been developed with increasingly reliable modeling of the interaction between the human pilot and the airplane. Traditionally, to simulate such manned flights using a computer, several different mathematical models [15–17] have been employed so as to represent the effects due to the human operator. All

these models have been developed to study the effect of only a single human pilot.

However, there are many situations in which we may be interested in studying the effect of not one pilot but a group of pilots with a range of skill, training, and experience levels [18]. For example, if a recommendation is to be made for a population of pilots as the result of a research study, a pilot model based on a single human operator cannot be used. The pilot model used in the study should be representative of the whole population of the pilots that will operate upon the recommendation. When a recommendation is drawn based on a single pilot model, it will be valid for that specific pilot; however, there is no guarantee that it will be effective for the other pilots with various levels of skill, training, and experience. Another example is when there is no a priori knowledge on what kind of pilot will be using the result of a research study or how exactly a pilot will behave in an unsettling situation. Hence, there is a need to develop a human pilot model that could, using an appropriate method, represent the effect of a group of pilots. One simple and efficient method to model a group of pilots is to incorporate a probabilistic approach that contains certain characteristic parameters used to signify such features as the skill, experience, and training of each pilot belonging to the group. By choosing suitable probability density functions for each of these parameters, the variation in skill set of the individual pilots can be included in the simulation study.

This paper presents the probabilistic approach as implemented in a microburst escape maneuver of a commercial airliner flown by a pilot. The Federal Aviation Administration (FAA)'s Windshear Training Aid [19] recommends that on recognizing an encounter with severe wind shear, the pilot should command maximum thrust and rotate the aircraft to an initial target pitch angle (TPA) of 15 deg. After the FAA's recommendation, a substantial research effort has been devoted to determining the effect of windshear on the aerodynamic characteristics [20–22] and flight modes [23], and to finding optimum escape strategies [24–35]. In [24,36,37], various suboptimal guidance strategies are compared. The common feature of the optimal escape trajectories in most studies has been, without excessive loss of kinetic energy or airspeed, to increase or to maintain the altitude in the case of aborted landing and to track a target trajectory in the case of takeoff and penetration landing. Zhao and Bryson, Visser, and Dogan and Kabamba [30,38–40] suggest that an initial descent may improve the safety of an escape maneuver. In this paper, the application of the probabilistic human factor modeling to the area of aircraft microburst encounter is specifically chosen due to the fact that the recommendation for the escape maneuver in the case of an unexpected encounter of a microburst during the landing approach is general for the entire population of the commercial airline pilots and the microburst encounter in the landing phase of the flight is usually unexpected, rare, and unsettling for the pilots because the aircraft is so close to the ground. The pilots may have a very large range of variation in skill, training, and experience regarding microburst encounters and the behavior of the pilots in this critical and dangerous flight condition may vary widely. However, the recommendation for such a flight condition needs to be general for every airline pilot.

The development of the PRM (Precision Runway Monitor) system [41] is an example where the development process is complicated by the fact that the parameters that characterize the events of the onset, detection, and resolution of a blunder during independently sequenced parallel approaches are statistical variables that take on a range of values with a characteristic distribution. The PRM was an effort to increase poor-weather capacity at airports having parallel runways and considered human factors by taking into account air traffic controller response times. Separate measurement and analysis efforts were carried out to provide realistic statistical distributions for each parameter including air controller reaction times. Then, evaluation of overall PRM system performance used the measured statistical distributions as inputs in estimating collision risk in the case of parallel approach blunders through Monte Carlo simulations. In [42,43], a prototype alerting system was developed using Monte Carlo simulations to assess the probability of a conflict over a range of free-flight traffic encounters. In [42], escape maneuvers are included as part of the probabilistic alerting analysis to ensure that sufficient maneuvering space is available to avoid conflict. The avoidance trajectories are evaluated probabilistically to account for uncertainty in flight crew response time and variability in their actions. Then, the likelihood of safely maneuvering out of the conflict is defined and used to determine the most favorable avoidance trajectories. In [43], Monte Carlo simulations are used to estimate conflict probability as a function of intruder position, heading, and speed. Further, the probability of conflict along potential avoidance trajectories is used to indicate whether adequate space is available to resolve a conflict. Similarly, in this paper, a probabilistic method is adapted to develop representative models of a group of pilots based on a single pilot model for the purpose of quantifying sensitivity of various microburst escape guidance strategies to human pilot factors. Every single pilot model has a set of parameters to characterize certain aspects of human behavior in interactive man–machine systems. The approach used in this paper is based on the fact that each parameter in the pilot model has a stochastic variation in a group of pilots and thus can be modeled as a random variable with a specified probability density function (PDF). The pilot parameters that are treated in this paper as random variables are limited to those that represent the ability of a pilot to execute a guidance strategy. The compensator dynamics are an exact representation of the intended control strategy and no uncertainty is considered in the pilots' understanding of the guidance strategy, which means that this paper models the human pilot factors in the inner-loop tracking of guidance commands. This is because the paper focuses on the parameters whose probabilistic distributions are easy to determine from flight or simulator data as opposed to those such as imperfection in cognitive understanding of guidance strategies. Further, this paper is aimed at quantifying the level of difficulty for pilots to safely implement three specific guidance strategies in an unsettling flight condition, or, in other words, the sensitivity of the three guidance strategies to human factors. Once the parameters are selected to be considered as random variables, their probability distributions are used in a Monte Carlo analysis to estimate the probability of specified performance metrics to compare the three guidance strategies. The random variables and the PDFs used in this paper are chosen based on the results available in the literature and the intuition of the authors. No attempt has been made to determine the true probabilistic nature of the parameters based on a group of pilots in the current work and this is left as a topic for future work. This paper focuses on the conceptual proof of the effectiveness of the method under the assumption that the random variables and their PDFs are scientifically obtained based on a sample of real pilots.

The remainder of the paper is organized as follows. The single human pilot model is explained in Sec. II. In Sec. III, a probabilistic method to develop a model for a group of pilots based on the single pilot model is presented. An application to microburst escape maneuver to evaluate the efficiency of the probabilistic human pilot model is explained in Sec. IV. Section V describes the Monte Carlo simulations. The results and discussion are given in Sec. VI. Finally, Sec. VII completes the paper with some concluding remarks and recommendations for future work.

II. Single Human Pilot Model

In this paper, a probabilistic human pilot model is developed based on a single pilot model to represent a group of pilots. Thus, a description of the single pilot model is given first, in this section. The single human pilot models used in the literature are divided broadly into two categories, namely, frequency domain models and time domain models. The human pilot model used in this paper is in the latter category. In this paper, the effect of the human pilot model is applied to only one control input, namely, the elevator deflection. The throttle, aileron, and rudder deflection controls are considered to be the same for all the escape guidance strategies. This is because, during a microburst escape maneuver using the three guidance strategies compared in this paper, the longitudinal motion of the airplane is the most critical aspect of flight. Furthermore, note that the elevator deflection and the throttle setting are the main control inputs

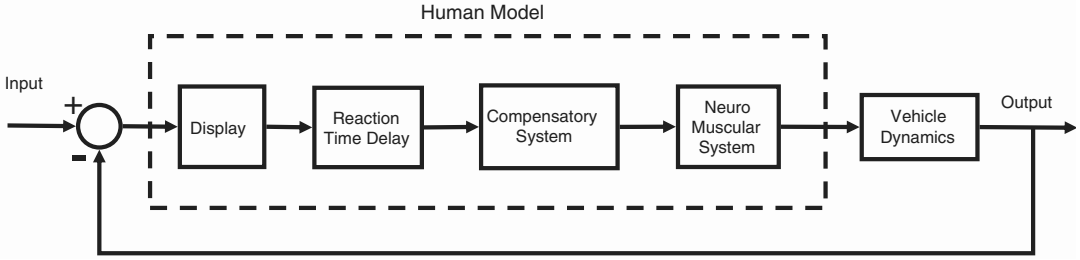

Fig. 1 Feedback structure of the pilot model and the systems.

for the longitudinal flight. Given the fact that the maximum thrust is applied during any escape maneuver, the only control variable left that the pilot should be adjusting is the elevator deflection. The overall structure of the pilot model in the form of feedback control is shown as a schematic block diagram in Fig. 1. In this figure, the equalization network is referred to as the compensatory system. The observation noise is treated together with the display component and the motor noise is studied in combination with the neuromuscular system. Traditionally, the pilot models are named based on the control theory used for the equalization or compensatory system. Because our study makes use of the nonlinear dynamic inversion (NDI) technique for the control design, the pilot model used in this paper may be referred to as "nonlinear pilot mode."

As seen in Fig. 1, the human pilot model consists of four different components.

A. Display Including Observation Noise

Display systems form the medium by which the pilot observes and interprets the instantaneous state of the aircraft. The pilots' decision is based on the combination of his experience and the readings sensed by the aircraft instruments such as airspeed indicator, altitude sensor, or visual observation of the external environment. There are various sources of error in the process of measuring and interpreting the actual aircraft states. For example, there could be instrument errors such as those due to the hardware sensitivity, calibration, etc., or, given perfect measurements from the instrument, observation error which deals with the errors in the pilot viewing and interpreting the output from the displays. Additionally there could be some unmodeled effects due to coupling with external environment and operating conditions. To sufficiently model these factors, a random term called the observation noise needs to be included in the human pilot model. The effects due to the instruments and the environment are treated to be the same for all the test cases and therefore the observation noise term is used primarily to study the effects of different pilots with varying ability to observe the measurements from the displays. The observation noise is modeled by a Gaussian white-noise process with a specified covariance [7]. The display error with observation noise is added to the plant error before operating it with the reaction time delay term [44].

B. Reaction Time Delay

In the real piloted aircraft flight, there is a finite amount of time involved in the pilot's eyes reading the signals from the displays, with these signals then being sent to the brain for processing and decision making, and finally for the control commands from the brain to be actually executed by the muscles. Such visual measurement time, sensory transportation time, and processing time (brain) can be approximated in the human pilot model by a reaction time delay term. The overall amount of time for the above processes depends upon the pilot's characteristics such as training, experience, and knowledge. The mathematical model of the reaction time delay is represented by $e^{-\tau s}$ where τ denotes the reaction time constant in seconds and s, the Laplace variable. However, because the exponential function is irrational, there is a need to approximate $e^{-\tau s}$ in terms of rational functions. The literature shows several Pade formulas to approximate the time delay using polynomial functions of various orders. Choosing higher order approximations might improve the accuracy although at the expense of computational efficiency. In this paper, the main focus is on developing a model for a group of pilots and not to achieve the best accuracy for a single pilot representation. Hence, for the sake of convenience, in our study, the first Pade approximation [45,46] given by

$$e^{-\tau s} \simeq \frac{1-\tau s/2}{1+\tau s/2} \tag{1}$$

is employed to represent the reaction time delay. The reaction time delay for a typical pilot is due to effects such as nerve conduction time, central processing time, and has been determined to be roughly about 0.15–0.30 s [7].

C. Compensatory System

The compensatory system, analogous to a controller in the feedback control system, forms the core of the human pilot model. It is responsible for deciding the necessary control action based on a certain control law. The other components of the human pilot model act upon the input/output signals to/from the compensatory system so as to represent the effects that are experienced in practice due to the presence of a human pilot. Because the controller is considered to be a compensatory system [4], the plant error is the only signal constituting the input to this system. The controller has four modes, a different combination of which is used in three different escape guidance strategies in a microburst encounter.

1. *Pitch Angle Controller*

The NDI technique is used in designing the controller for the elevator to track the commanded pitch angle θ_c. The control law for the elevator deflection is

$$\delta_e = \frac{1}{f_{\theta_e}}(u_\theta - f_{\theta_0}) \tag{2}$$

where

$$u_\theta = \ddot{\theta}_c - K_{\theta_1}(\dot{\theta}-\dot{\theta}_c) - K_{\theta_2}(\theta-\theta_c) \tag{3}$$

$$f_{\theta_e} = \frac{\cos\phi}{I_{yy}} f_{\mathcal{M}_e} \tag{4}$$

$$\begin{aligned} f_{\theta_0} = {} & \frac{\cos\phi}{I_{yy}}[(I_{zz}-I_{xx})pr + I_{xz}(r^2-p^2) + f_{\mathcal{M}_0}] \\ & - \frac{\sin\phi}{\Delta_1}(\Delta_2 pq + \Delta_3 qr + I_{xz}\mathcal{L} + I_{xx}\mathcal{N}) \\ & - (q\sin\phi + r\cos\phi)[p + (q\sin\phi + r\cos\phi)\tan\theta] \end{aligned} \tag{5}$$

and

$$f_{\mathcal{M}_e} = \tfrac{1}{2}\rho\mathcal{S}\bar{c}V^2 C_{\mathcal{M}_{\delta_e}} \tag{6}$$

$$f_{\mathcal{M}_0} = \frac{1}{2}\rho\mathcal{S}\bar{c}V^2\left(C_{\mathcal{M}_\alpha}\alpha + C_{\mathcal{M}_q}\frac{\bar{c}}{2V}q_{\text{ref}}\right) + \Delta z T \tag{7}$$

$$\Delta_1 = I_{xx}I_{zz} - I_{xz}^2 \tag{8}$$

$$\Delta_2 = I_{xz}^2 - I_{xx}I_{yy} + I_{xz}^2 \tag{9}$$

$$\Delta_3 = I_{xz}(-I_{xx} + I_{yy} - I_{zz}) \tag{10}$$

Note that the aircraft equations of motion that this control law is based on have (p_{rel}, q_{rel}, r_{rel}), the angular velocity components of the aircraft relative to air. However, in the above control algorithm, instead of (p_{rel}, q_{rel}, r_{rel}), (p, q, r), the angular velocities of the aircraft relative to ground, are used because the pilot can only have access to or sense (p, q, r) during the escape maneuver. Because the NDI technique is used in the controller design, the pitch dynamics in the closed loop response behaves as a linear second-order system as long as the elevator deflection is not saturated.

$$(\ddot{\theta} - \ddot{\theta}_c) + K_{\theta_1}(\dot{\theta} - \dot{\theta}_c) + K_{\theta_2}(\theta - \theta_c) = 0 \tag{11}$$

The design procedure and the other details of this controller can be found in [39,47].

2. Climb-Rate Controller

This controller computes the required pitch angle, which is used as the commanded pitch angle for the pitch angle controller, that results in the desired climb rate. The control law is obtained by dynamic inversion of the translational kinematics equation for the altitude rate:

$$\theta_c = \alpha + \sin^{-1}\left(\frac{\dot{h}_c}{V}\right) \tag{12}$$

where negative $\dot{h}_c$ implies descent.

3. Altitude-Hold Controller

This is a PID controller that calculates the commanded pitch angle to maintain the commanded altitude:

$$\dot{\theta}_c + K_{u_1}\theta_c = K_{u_0}u_c \tag{13}$$

where

$$u_c = K_{p_h}\Delta h + K_{d_h}\Delta\dot{h} + K_{i_h}\int_0^t \Delta h \, \mathrm{d}\tau \tag{14}$$

and K_{p_h}, K_{d_h}, K_{i_h}, K_{u_0}, and K_{u_1} are the gains, and $\Delta h = h_c - h$. Again, see [39,47] for details.

4. Stall Prevention Mode

This mode is used to represent the behavior of pilots pitching down the airplane to reduce the angle of attack and to increase the airspeed to prevent the aircraft from stalling in an escape maneuver [19]. In this study, a stall prevention mode is triggered when the airspeed drops less than a specified stall speed and the angle of attack exceeds a specified maximum limit $\alpha_{\max}$. When these two conditions occur at the same time, the pilot immediately initiates the preventive action of reducing the pitch angle to 70% of the current pitch angle and keeps it there until both airspeed and angle of attack are no longer within their respective stall region.

D. Neuromuscular Dynamics System Including Motor Noise

Each pilot has his/her own way of responding to the same flight condition. For example, to achieve precise tracking of a reference flight attitude, while one pilot may exert smooth control inputs by moving the stick gently, another pilot might force the stick very hard [44] to accomplish the same specific task. This dependency of the closed loop system response on the pilot can be represented in the human pilot model by means of a neuromuscular dynamics system that characterizes the personality, skill, knowledge based on training, and experience of each pilot. Specifically, the neuromuscular dynamics system is used to express the changes in the position of the hands and the length of the muscles in terms of the force due to the acceleration of the mass of the hands, and spring stiffness and the damping characteristics of the muscles [48]. In the literature, even though the approximation of the neuromuscular dynamics as a second-order system [6] has been used for greater accuracy, a first-order approximation [6,7,49] is considered to be sufficient for most analytical studies. Hence, in our work, the muscular response has been modeled as a first-order dynamic system with a time constant of 0.1–0.2 s [50]. The mathematical model of the neuromuscular system is

$$\frac{1}{\tau_N s + 1} \tag{15}$$

Additionally, we have one more term called the motor noise, which represents natural factors such as physical stability, mental stress, and intensity of concentration. The motor noise results in an overshoot or undershoot in the neuromuscular response of the human operator. This type of error depends upon the emotional and mental state of the pilot during an unsettling flight condition such as a microburst escape maneuver. In this study, the motor noise can be interpreted as the event where the pilot attempts to move the stick to adjust the control surfaces. The error occurs when the pilot makes oscillations due to his or her attempts to control the aircraft. This error affects the elevator deflection but is small compared with the range of the admissible elevator deflection. This error, called motor noise, is represented as a zero-mean Gaussian white noise with spectral density proportional to the mean square operator output [7,8]. Thus, in our study, modeling the effect of a single human pilot's behavior on the aircraft controller has been accomplished by adding the components, namely, the reaction time delay, neuromuscular system, observation noise, and motor noise to the compensatory system.

III. Probabilistic Pilot Model

As stated earlier, a simple single pilot model may not be sufficient to make decisions or recommendations in cases of research study that might involve pilots with a wide variation in response characteristics. Hence, in such cases, there is a need to incorporate a model for not a single pilot, but a whole group of pilots. The key discriminator between a single pilot model and a model for a group of pilots is the presence of the ability to incorporate the variation of the personal attributes and skills of the individual pilots in the group. A probabilistic approach is efficient in this regard because, this way, the variation of skills between the individual pilots or the likelihood of variation in the skills of a single pilot in an unsettling situation can be expressed as random variables with suitable probability density functions.

In the single pilot model explained in the previous section, the parameters that will vary depending on the level of a pilot's training, experience, skill, mental and emotional state are the following:

1) the time constant τ in the reaction time delay model,

2) the time constant τ_N in the neuromuscular dynamic system model,

3) the noise power in the observation noise, and

4) the noise power in the motor noise.

A necessary step in the construction of a probabilistic pilot model is to be able to determine the probability characteristics of these parameters as probability density functions. Because of the lack of available literature that can provide statistical properties of a group of pilots or statistical variations of a single pilot characteristics in terms of probability density functions, the following ad hoc approach is adopted to determine the probability density functions so that the benefits of the probabilistic pilot model approach can be demonstrated. The first step in this approach is to find a suitable

probability density function that can characterize probabilistic variation of the four pilot parameters. Note first that the smaller the parameters are, the better the pilot is considered to be because it would take him less time to think of (reaction time delay) and initiate (neuromuscular dynamics) a reactive action, and, during the execution of the action, the distraction in his ability to observe (observation noise) and perform (motor noise) would be smaller. However, in real life, the probability of finding the best performing pilot is very small. On the other hand, the probability of finding a pilot with the worst performance is small as well. Further, because we do not know how badly the pilot may react, the values of the parameters, representing the worst performance, should go to infinity, even if with very small probability. In general, however, most of the pilots should perform similarly and at the average. In this paper, this intuition is represented by using a Rayleigh PDF [51] for each of the "random" variables. However, for a reason that will be explained in the following paragraph, a shifted version of Rayleigh distribution is used. The PDF of the shifted Rayleigh random variable is

$$f(x) = \frac{(x - x_0)}{\sigma^2} e^{-(x-x_0)^2/2\sigma^2} u(x - x_0) \tag{16}$$

where $u(x)$ is the unit step function, whose value is 1 for $x \geq 0$ and 0 for $x < 0$, and x_0 represents the amount of shift.

As the above equation indicates, the shifted Rayleigh PDF has two parameters, σ and x_0. The next step, then, is to determine these parameters for each of the four random variables of the probabilistic pilot model. This is done by first determining the corresponding ranges, either as reported in the literature or by the intuition of the authors. First, σ for each random variable is selected such that its expected value is at the middle of the corresponding range. For example, based on the prior experience with the behavior of most human pilots, it is reported [7] that τ, the reaction time delay varying from 0.15 to 0.3 s, covers the entire range of pilots encountered in normal operating conditions. Further note that a pilot with zero τ would respond instantaneously, without any delay in his decision making for reaction, to any new flight situation. Obviously, this would be impossible even for the best pilot. Thus, the probability of τ taking a value of zero or very close to zero should be zero. Thus, the PDF representing τ is obtained by shifting the standard Rayleigh PDF by 0.05 as shown in Fig. 2.

By similar arguments, a shifted Rayleigh PDF is used to represent the probabilistic distribution of the time constant of the neuromuscular dynamic system (τ_N). This PDF is shifted by 0.03 and its expected value is in the middle of its corresponding range, which is reported [50] to be 0.1–0.2 s.

The third parameter is the variance of the observation noise, which is assumed to be a Gaussian random variable with zero mean. In other words, the probabilistic pilot model has a Gaussian observation noise

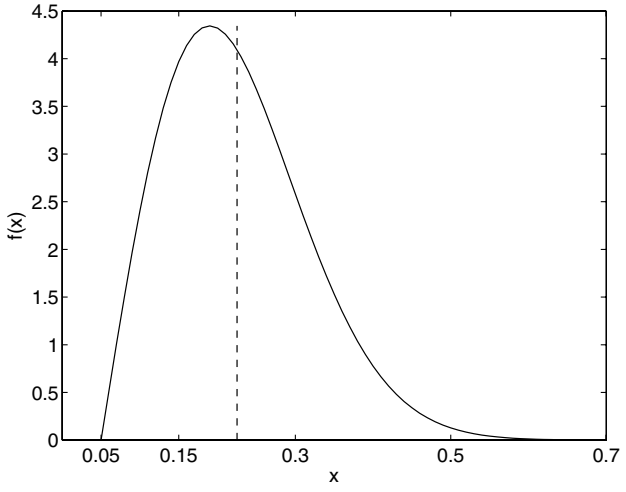

Fig. 2 Shifted Rayleigh PDF for the time constant in the reaction time delay.

Table 1 Shift amount, expected value, and σ parameter of Rayleigh distribution for the random pilot parameters

Parameter	Unit	x_0	$E[\cdot]$	σ
τ	s	0.05	0.225	0.1396
τ_N	s	0.03	0.15	0.0957
n_{oa}	m^2	0	9	7.181
n_{ot}	deg^2	0	0.16	0.1277
n_{ot}	deg^2	0	0.16	0.1277

with a variance that is a Rayleigh random variable. In this paper, the state variable measurements considered are those of the pitch angle or altitude depending upon the type of escape guidance strategy studied. Note that the variance of observation noise is represented by a standard Rayleigh PDF, without any shift. The variances of the observation noises in altitude and pitch angle are selected such that the respective standard deviations are equal to 2% of the corresponding limiting values considered for the simulation. Specifically, we consider that the normal operation range of the pitch angle commands is limited to 20 deg and the altitude of an airplane in a microburst encounter during landing varies between 0 and 150 m above the ground level. Therefore, the expected values of the variance of altitude (n_{oa}) and pitch angle (n_{ot}) observation noises are 9 m^2 and 1.6 deg^2, respectively.

The last parameter varied to model a group of pilots is the variance of the motor noise, which is also assumed to be Gaussian random variable with zero mean. The limits of the motor noise depend on the training, experience, and the emotional stability of the pilot. In all the escape guidance strategies, the control action is achieved by adjusting the elevator deflection. Thus, elevator deflection is used to represent the pilot's motor action. The amount of elevation deflection oscillation induced by the pilots encountering a microburst would be very small for highly skilled pilots with great mental composure as against those with little experience or poor temperament. As in the cases of observation noises, the variance of the motor noise (n_m) is considered to be a Rayleigh random variable, and its expected value is selected such that the standard deviation is 2% of the maximum elevator deflection allowed, 20 deg in this paper. Table 1 summarizes the statistical properties of the random pilot parameters. Note that all the random variables have Rayleigh PDF whereas the last three are the variances of Gaussian white noises with zero mean.

IV. Application to Microburst Escape Maneuver

In our research analysis, we apply the probabilistic approach to study the effect of human factors in controlling an airplane so as to escape a microburst using three different guidance strategies. The objective of this study is to determine the best guidance strategy in the sense of safety and robustness against human factors among the three for escaping from a microburst.

A. Microburst

A microburst is a small downburst with its outburst, damaging winds extending only 4 km or less. In spite of its small horizontal scale, an intense microburst may induce damaging winds as high as 75 m/s. By virtue of its small size and its short life of less than 10 min, a microburst often escapes detection by non-Doppler radars or ground-based anemometers. Consequently, an aircraft at low altitude may encounter a microburst unexpectedly. The small spatial scale of a microburst converts into steep wind shear gradient experienced by the penetrating aircraft, and fast changes in wind vector, perhaps well in excess of the inertial capabilities of the airplane [47]. Mathematically, an axisymmetric, three-dimensional and stationary microburst [47] can be modeled in terms of the induced radial and vertical wind velocities at any point in the three-dimensional space as

$$W_r = f_r \cdot \left\{ \frac{100}{[(r - D/2)/200]^2 + 10} - \frac{100}{[(r + D/2)/200]^2 + 10} \right\} \tag{17}$$

$$W_h = -f_h \cdot \left[\frac{0.4h}{(r/400)^4 + 10}\right] \tag{18}$$

where

$$r = \sqrt{(x - x_c)^2 + (y - y_c)^2} \tag{19}$$

Using polar coordinates, the horizontal wind components W_x and W_y can be readily related to the radial wind component W_r as

$$W_x = \cos\psi_w W_r(r), \qquad W_y = \sin\psi_w W_r(r) \tag{20}$$

B. Aircraft Model

The 6 degree-of-freedom (DOF), rigid-body aircraft model used in this paper is the same as that presented in [47]. This model consists of 13 first-order nonlinear equations including engine dynamics, saturation, and rate limit of the actuators. The nonlinear equation incorporates the effect of wind components and wind gradients on the translational and rotational motion of the aircraft.

C. Initiation of Escape Maneuvers in Approach Landing

In all cases, simulations are started while the airplane is on a landing approach. The airplane continues to descend while the F factor is monitored using data obtained from a reactive microburst detection system. F factor quantifies the effect of windshear, due to microburst in this study, on airplane performance as an effective reduction in available excess thrust-to-weight ratio due to horizontal and vertical shears and downdrafts. Once the F factor exceeds the prespecified threshold value, the pilot aborts the landing and starts an escape maneuver based on one of the three guidance strategies. The details of this procedure can be found in [39,47].

D. Escape Guidance Strategies

Three escape guidance strategies [47] are compared in terms of their safety and insensitivity to human factors. 1) With the pitch guidance strategy, the pitch angle is commanded to be 15 deg once the escape maneuver is initiated and is then maintained as long as the angle of attack is less than its maximum allowable limit $\alpha_{\max}$. This strategy is recommended by the FAA in the Windshear Training Aid [19]. 2) The dive guidance strategy initiates the escape maneuver with a 0 deg pitch angle command which is maintained until the aircraft descends to the commanded altitude h_c. Once the commanded altitude is reached, the commanded pitch angle is increased to 15 deg. As for the pitch guidance strategy, the target pitch angle commands are maintained at either 0 or 15 deg provided the angle of attack is less than $\alpha_{\max}$. 3) In the altitude guidance strategy, there are three modes involved. The first mode, the climb/descent rate mode, directs the aircraft from the original altitude at the time of initiation of the escape maneuver to the commanded altitude h_c. During this mode, the commanded rate of descent is not constant but scheduled based on the altitude difference between the current altitude to the commanded one in such a way that a smaller descent rate is commanded as the altitude gets closer to the commanded altitude and the commanded descent rate becomes zero when the actual altitude is at the commanded one. Once the aircraft is at the commanded altitude, the pilot switches to the altitude-hold mode, in which he/she flies the aircraft at this constant recovery altitude until the high shear region of the microburst is overcome. Once the aircraft exits the wind field of the microburst, the third mode, namely, the climbing mode, is triggered and the target pitch angle is set to 15 deg. In all three guidance strategies, when the conditions occur, the current strategy is immediately abandoned and the stall prevention mode is triggered. Once the danger of stall is cleared, the normal strategy takes over the control. Note that in the case of the altitude guidance strategy, if the aircraft has descended lower than the commanded altitude as a result of the stall prevention maneuver, the climb/descent rate mode is used, this time, to ascend the aircraft to the commanded altitude. Figure 3 illustrates the elements of the control modes and their relations.

Figure 4 shows the time histories of altitude in escape maneuvers with three guidance strategies. Note that the airplane is on the landing path until about 10 s and then escape maneuvers are triggered. In all three cases, the airplane is exposed to the same moderate microburst ($f_r = 2$ and $f_h = 2$), and commanded altitude for dive and altitude guidance maneuvers is 40 m.

E. Incorporation of Human Factors into the Simulation

Reaction time delay occurs at every instant when the pilot executes a decision. In the case of a microburst escape maneuver, the first instant is when the landing is aborted and an escape maneuver is triggered. In aircraft equipped with a reactive windshear warning system, a warning is issued in the cockpit when the F factor exceeds a threshold. Then, the pilot should trigger an escape maneuver. The time it takes for the pilot to initiate the escape maneuver once the warning is issued is the pilot reaction time delay. In the simulation, this is implemented by delaying the F-factor signal and switching to the escape mode when the delayed F factor exceeds the threshold. Another instant of reaction time delay is when the pilot should initiate a stall prevention maneuver. From the time when a stall warning is issued in the cockpit, it takes the amount of delay time for the pilot to start the stall prevention maneuver. In the simulation, the risk of stall is detected based on airspeed and angle of attack as explained in Sec. II.C.4. The pilot reaction delay is implemented by delaying the

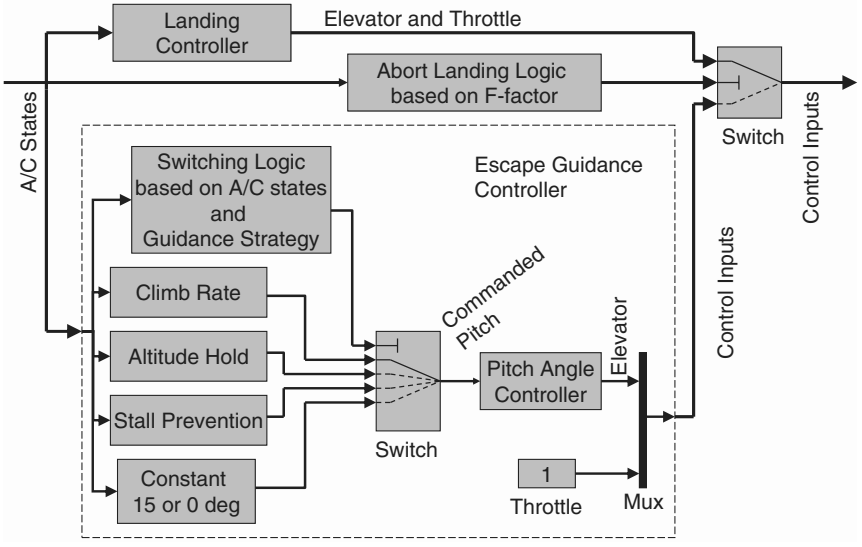

Fig. 3 Block diagram that shows the elements of the control system and their relations.

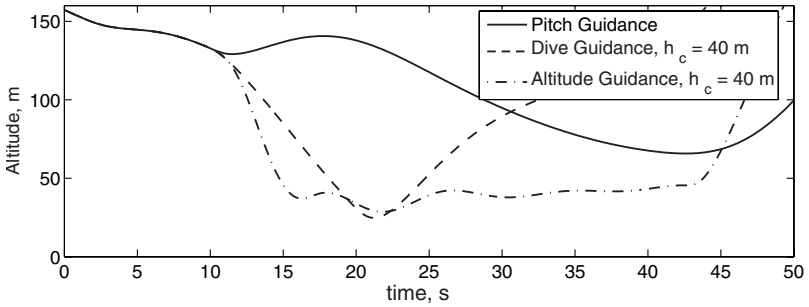

Fig. 4 Time histories of altitude with three escape guidance strategies.

flag that is used to indicate when the simulation should switch to the stall prevention mode. The same delayed flag is used to simulate the delay in pilot action to switch back to the escape maneuver when the risk of stall is over. Similarly, in the case of altitude guidance, the reaction delay in pilot switching between the three modes is simulated by delaying the corresponding flags. Note that discrete delay function is used to delay discrete signals such as flags as the Pade approximation is used to delay continuous signals such as the F factor. In the case of pitch and dive guidance, the delay in the pilot executing the commands to change the pitch angle is simulated by delaying the commanded pitch angle before sent, as input, to the pitch angle controller. Note, from Fig. 3, that, in altitude guidance, the pilot executes each of the three modes through controlling the pitch angle. Thus, the commanded pitch angle is delayed in this escape guidance strategy as in the other two.

The neuromuscular dynamics and motor noise are simulated by superimposing Gaussian noise with a specified variance on the elevator deflection computed by the pitch angle controller and then passing the resultant signal through a first-order transfer function as stated in Sec. II.D.

Display and observation noise is simulated by superimposing Gaussian noise with a specified variance on either pitch angle or altitude depending on the guidance strategy used. In the case of pitch guidance or dive guidance, noise is added to the pitch angle because the goal of the pilot is to follow the commanded pitch angle and thus the pitch angle is observed. On the other hand, because the altitude guidance focuses on the altitude response of the airplane, and thus the altitude is closely observed, observation noise is added to altitude.

V. Monte Carlo Simulation

In the previous sections, a single pilot model based on a nonlinear design technique is developed. Then, the parameters of this single pilot model, characterizing different aspects of human pilot behavior and reaction, are defined to be random variables with specified probability density functions. This is done to represent a group of pilots instead of a single one or to take into account the fact that it is not deterministically known what kind of pilot will fly the airplane or how he would react to a very dangerous and unsettling flight condition such as a microburst encounter in landing phase. A comparison between the three different guidance strategies is made based on the most important factor in a microburst escape maneuver, how much lost altitude the airplane will experience, or how close it will fly to the ground. This factor is quantified by the minimum altitude the airplane flies during the escape maneuver. Because the trajectory of the airplane and thus the minimum altitude depend on the nature of the microburst and the pilot's behavior and reaction during the escape maneuver, the minimum altitude becomes a random variable given the fact that both the microburst and pilot parameters are random variables. Hence, to be able to compare the escape guidance strategies, the probability density function or at least some statistical properties of minimum altitude should be determined. However, this is not possible analytically because the minimum altitude cannot be formulated as an explicit function of the microburst and pilot parameters, because it requires the analytical solution of the differential equations of motion of the aircraft-pilot system. Even if an explicit expression is obtained, it would be too complicated to determine the probability density function of the minimum altitude using the probability density functions of the random microburst and pilot parameters. Therefore, a numerical solution technique called Monte Carlo simulation [52] is adopted to obtain a numerical approximation of the cumulative distribution function (CDF) of the minimum altitude.

The CDF could be used to represent the likelihood of the event that the minimum altitude will be less than or equal to an altitude of interest. It also represents the probability of crash. The frequency of occurrences of those events can be computed by the Monte Carlo estimation of the cumulative distribution function of minimum altitude [39] according to the specified PDFs. The Monte Carlo method is employed by generating random numbers. The simple structure of Monte Carlo algorithms makes the method extremely convenient for multiprocessor (parallel) computation.

In our simulation study, the minimum altitude $h_{\min}$ depends on the initial condition ($\underline{z}_0$) at which the aircraft enters the microburst, the parameters of the microburst ($\underline{\theta}$), and the pilot implementing an escape guidance strategy ($\underline{K}$). Hence,

$$h_{\min} = h_{\min}(\underline{z}_o, \underline{\theta}, \underline{K}) \tag{21}$$

Assume that $\underline{z}_o$ is given and that $\underline{\theta}$ and $\underline{K}$ are continuous random vectors with a given joint probability density function, $\underline{f}_{\theta K}(\underline{\theta}, K)$. Because $h_{\min}(\underline{z}_o, \underline{\theta}, \underline{K})$ is a function of two random vectors, it is also a random variable. Thus, we can define its cumulative distribution function.

$$F_{h_{\min}}(h) = \Pr(h_{\min} \le h) \tag{22}$$

which tells us the probability of having $h_{\min}$ less than or equal to h. This probability or the cumulative distribution function of $h_{\min}$ can be computed from

$$F_{h_{\min}}(h) = \Pr(h_{\min} \le h) = \int_{D_\theta}\int_{D_K} I(\underline{\theta}, \underline{K}, h)\underline{f}_{\theta K}(\underline{\theta}, \underline{K})\,\mathrm{d}\underline{\theta}\,\mathrm{d}\underline{K} \tag{23}$$

where $I(\underline{\theta}, \underline{K}, h)$ is the indicator function defined as

$$I(\underline{\theta}, \underline{K}, h) = \begin{cases} 1, & \text{when } h_{\min} \le h \\ 0, & \text{otherwise} \end{cases} \tag{24}$$

Note that

$$F_{h_{\min}}(0) = \Pr(h_{\min} \le 0) \tag{25}$$

is the probability of crash. Also note that the probability of crash depends explicitly on $\underline{K}$ as well as $\underline{\theta}$. In this paper, the microburst parameters are

$$\underline{\theta} = [f_r, f_h, D, x_c, y_c]^T \tag{26}$$

and the human pilot parameters are

$$\underline{K} = [\tau, \tau_N, \{n_{oa} \mid n_{ot}\}, n_m]^T \tag{27}$$

Note, as stated in Sec. IV.E, that in a Monte Carlo run, either n_{oa} or n_{ot} is used depending on the guidance strategy of that run.

In this study, the marginal density functions f_{f_r} and f_{f_h} are assumed to be Rayleigh density functions [the Rayleigh density functions are used to fit the statistical data from the joint airport weather studies (JAWS)], and f_D, f_{x_c}, and f_{y_c} are uniform probability density functions [47]. In the Monte Carlo simulations, we have the following expected values for the microburst parameters:

$$E[f_r, f_h, D, x_c, y_c] = [2,\ 2,\ 2000,\ -1500,\ 0] \tag{28}$$

As stated earlier, the expected values of the human parameters are

$$E[\tau, \tau_N, \{n_{oa} \mid n_{ot}\}, n_m] = \left[0.2250, 0.15, \left\{9 \middle| 1.6\frac{\pi}{180}\right\}, 1.6\frac{\pi}{180}\right] \tag{29}$$

Because Monte Carlo simulation is used to calculate estimates of unknown quantities such as probability of crash, the quality of the estimates is evaluated with confidence intervals, which means a statement of the form

$$\Pr(L < R < U) \geq 1 - \delta \tag{30}$$

where $\delta \in (0, 1)$ is the confidence parameter, and L and U represent lower and upper bounds of the confidence interval, respectively, for the unknown, R [39,47]. The lower and upper bounds are computed using the approximation method of Anderson and Burstein [53,54]. This method is based on the fact that the Poisson distribution approximates the binomial distribution.

VI. Results and Discussion

The objective of the Monte Carlo simulation analysis in our study is to evaluate the effect of human factors on the performance of three different guidance strategies for escaping a microburst and thereby to identify the strategy that is least sensitive to the human factors. We intend to make the inference from the analysis to be general in terms of the commanded altitude, the variation in microburst strengths and locations, and also the actual behavioral attributes of any individual human pilot. In other words, the conclusion derived from our analysis is based on a variety of microburst encounters that are handled by a variety of human pilots with various levels of skill, training, and experience.

After running the Monte Carlo simulations, by implementing the strength and location of the microburst encountered and the characteristic parameters of the human pilot model as random variables, the probabilities of crash and the cumulative distribution function of minimum altitude for three different guidance strategies are obtained along with the confidence intervals. For the calculation of confidence intervals, the value of the confidence parameter [47] is taken to be 0.05, which means that the upper and the lower limits determine 95% confidence intervals. In this study, no effort was made to tighten the confidence intervals because the goal was only to achieve confidence limits small enough to have conclusive comparisons between the escape strategies. Thus, about 500 Monte Carlo runs were performed per escape guidance strategy per commanded altitude. The Monte Carlo simulations are run in two cases: 1) the escape guidance strategies implemented by pilots and 2) the escape maneuvers are executed with controllers without human pilot interference.

Figure 5 shows the variation of the probability of crash with commanded altitude for three different guidance strategies, implemented by pilots. Because the commanded altitude is not a strategy parameter for the pitch guidance strategy, the probability of crash for this strategy is represented as a constant line. It is noted that altitude guidance results in highest probability of crash in the whole range of commanded altitudes considered. For altitude guidance, the lowest probability of crash is observed with a commanded altitude of 100 m. Further note that probability of crash with altitude guidance has a local minimum at 30 m commanded altitude and increases very rapidly as the commanded altitude decreases while staying approximately the same as the commanded altitude increases. Note also that altitude guidance with higher commanded altitudes is more likely to require a stall prevention maneuver and thus the pilot is less likely to be able to fly the airplane at the commanded altitude. Dive guidance gives the lowest probability of crash with any commanded altitude higher than 20 m. The lowest probability of crash is obtained with dive guidance with commanded altitude 40 m.

Figure 6 shows the CDF of $h_{\min}$ of pitch, dive with 40 m commanded altitude, and altitude guidance with 30 and 100 m commanded altitudes. Note that the information about the probability of crash (shown in Fig. 5) for a particular guidance strategy can also be deduced from the CDF of $h_{\min}$ (shown in Fig. 6) by observing the value of CDF at zero altitude for the respective guidance strategy. CDF curves obviously carry much more information than just the probability of crash; for any given altitude, it gives the probability of the airplane descending lower than that altitude during an escape maneuver. Figure 6 clearly shows that dive guidance with 40 m commanded altitude gives the lowest probability of descending lower than 20 m. Thus, only when the altitude range of interest is from 0 to 20 m, the dive guidance with 40 m commanded altitude seems to be the most favorable guidance strategy. However, note that pitch guidance has the smallest CDF for altitudes higher than 20 m. For example, if a guidance strategy is sought to have the lowest probability of descending below 40 m, then the pitch guidance becomes more favorable. Namely, the probability of having a minimum altitude less than 40 m is 0.33 with pitch guidance, 0.45 with altitude guidance of $h_c = 100$ m, 0.99 with dive guidance of $h_c = 40$ m, and 1 with altitude guidance of $h_c = 30$ m.

Based on the analysis of Figs. 5 and 6, the dive guidance would seem to be the most favorable in terms of probability of crash and probability of descending below 20 m. For altitudes higher than 20 m, pitch guidance is most favorable based on the smallest CDF. This conclusion is different from the results obtained in [39,47] where the altitude guidance with the appropriate commanded altitude seemed to be safer. The current study improves over [39,47] in three areas: 1) aborting landing and initiating an escape maneuver are simulated in this work while Dogan and Kabamba [39,47] start simulations at the initiation of escape maneuvers and thus ignore the

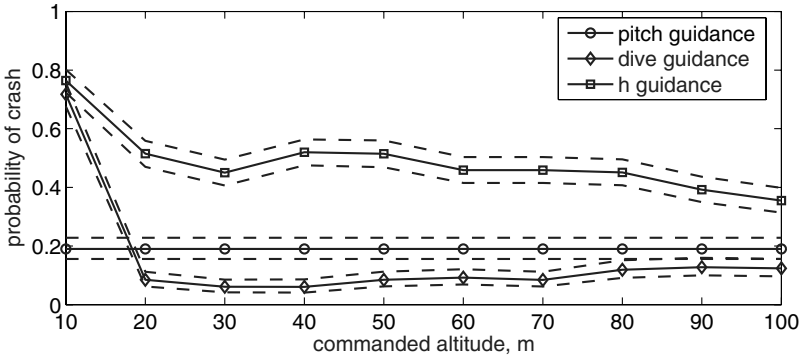

Fig. 5 Probability of crash with the three guidance strategies implemented by pilots. 95% confidence limits are shown with thin dashed lines.

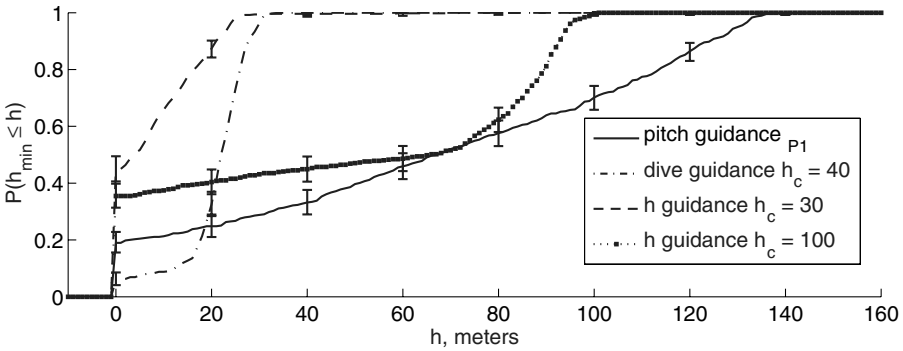

Fig. 6 CDF, $P(h_{\min} \leq h)$, of the three guidance strategies that show the lowest probability of crash. I bars are used to show the size of the 95% confidence intervals.

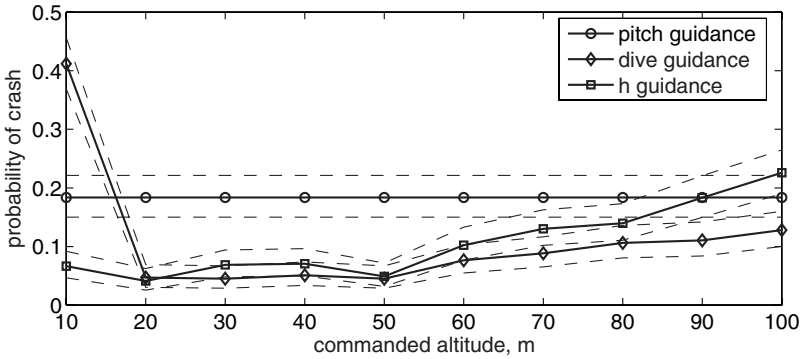

Fig. 7 Probability of crash with the three guidance strategies without human factors. 95% confidence limits are shown with thin dashed lines.

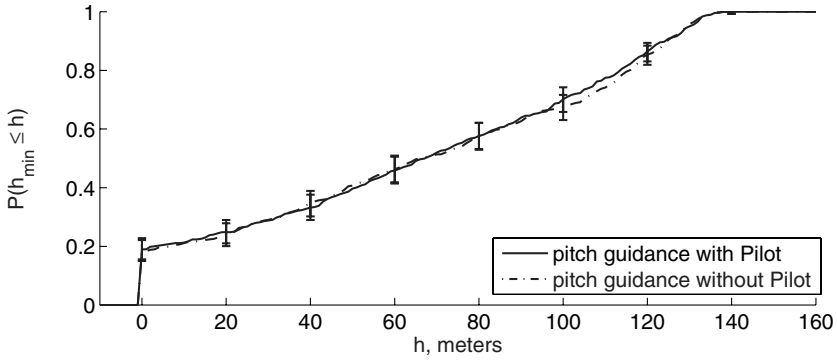

Fig. 8 CDF, $P(h_{\min} \leq h)$, of pitch guidance with and without human effects. I bars are used to show the size of the 95% confidence intervals.

transition. 2) Stall recovery maneuver is incorporated here but Dogan and Kabamba [39,47] do not attempt to recover from stall and consider it as a crash. 3) The main difference here is the consideration of human factors in escape guidance strategies. The first two differences alone do not significantly change the conclusion of [39,47] as the probabilities of crash curves versus commanded altitudes for the three guidance strategies without human factors are illustrated in Fig. 7.

Thus, in the remainder of this section, the sensitivity of the guidance strategies to human factors will be investigated by comparing the Monte Carlo simulation results from the two cases, with 1) pilot flying the airplane and 2) the controller implementing the escape guidance strategy. As seen in Fig. 8, CDFs of $h_{\min}$ with pitch guidance are very close to each other regardless of whether the probabilistic human pilot model is incorporated into the simulation. Thus, it can be inferred that the sensitivity of pitch guidance to human pilot effects is very small. In other words, the outcome of an escape maneuver using pitch guidance does not depend on the pilot, but on the microburst encountered.

Figure 9 shows that the effect of the human pilot on microburst escape maneuvers when the dive guidance is followed. The probability of crash with human pilot effects is slightly higher than that without human factors, especially with commanded altitudes lower than 20 m. Note that higher probability of crash means that the safety of the dive guidance is worsened if it is implemented by pilots. For commanded altitudes higher than 20 m, the probability of crash stays statistically the same. The divergence of the probability of crash with and without human pilot factors quantifies the sensitivity of the dive guidance to human pilot factors. Figure 9 shows that with lower commanded altitudes, the dive guidance is slightly sensitive to human pilot effects.

Figure 10 shows, in the case of altitude guidance, the dramatic degradation of safety when implemented by pilots and the increase of sensitivity to human effects as commanded altitude decreases. Without human factors, altitude guidance may be considered to enhance safety as commanded altitude decreases. However, Fig. 10 clearly shows, by the divergence of the two probability-of-crash curves, that the altitude guidance is very sensitive to human factors and results in a much worse performance as commanded altitude decreases.

Figure 11 presents the altitude guidance response trajectories in three different microburst encounters to illustrate the effects of

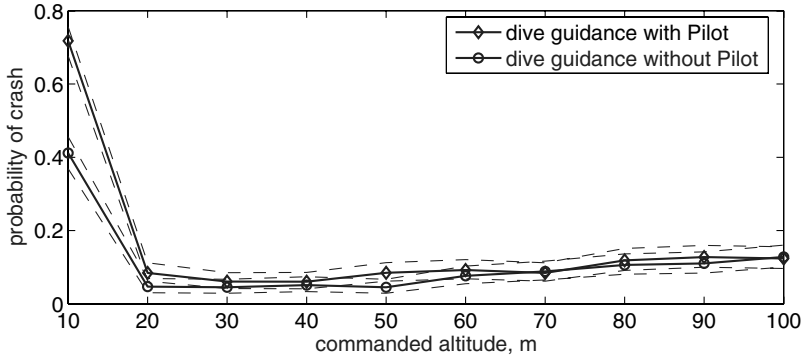

Fig. 9 Probabilities of crash with dive guidance with and without human effects. 95% confidence limits are shown with thin dashed lines.

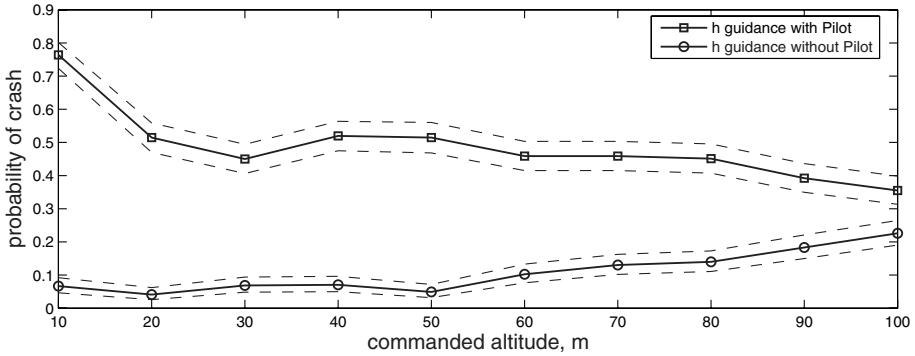

Fig. 10 Probabilities of crash with altitude guidance with and without human effects. 95% confidence limits are shown with thin dashed lines.

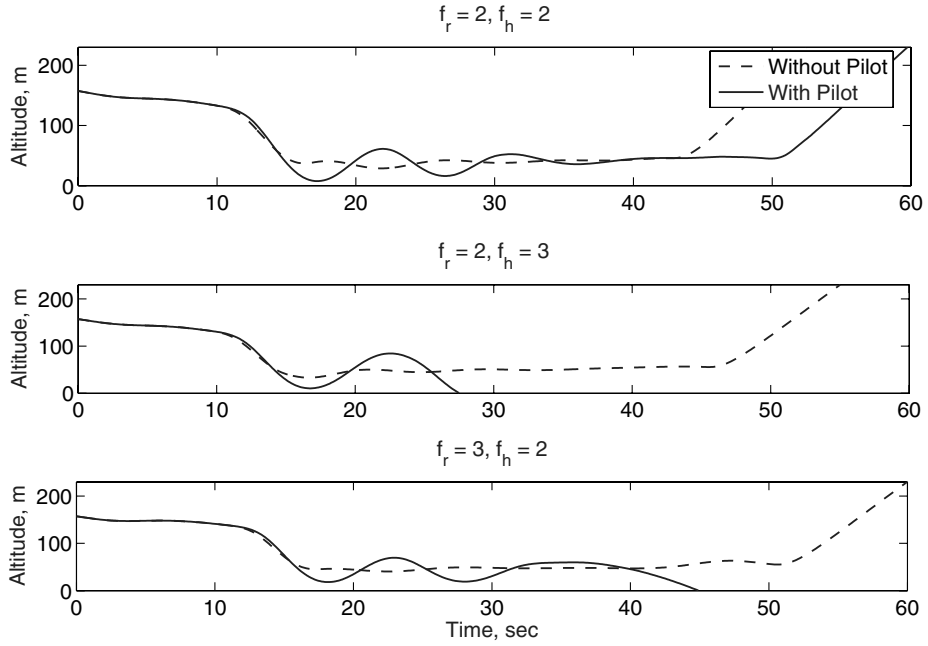

Fig. 11 Comparison of *h*-guidance response trajectories without and with pilot effects in three different microburst encounters. The radial and vertical strengths of the microburst are given at the title of each subfigure. The commanded altitude is 50 m. The values of the pilot parameters are at their corresponding expected values.

human pilot factors on increase in the probability of crash. The first case ($f_r = 2,\ f_h = 2$) shows that the human factors result in an undershoot of the commanded altitude and the pilot manages, after a few oscillations, to fly the aircraft around the commanded altitude. In the second case ($f_r = 2,\ f_h = 3$), the microburst has a stronger downdraft; thus the pilot cannot recover from the undershoot and crashes the airplane. In the third case ($f_r = 3,\ f_h = 2$), the microburst has stronger radial winds, that is, stronger head and tail winds. In this case, the pilot manages to recover from the undershoot and the airplane flies closer to the commanded altitude. However, the pilot has to initiate a stall recovery maneuver and unfortunately cannot recover from the crash due to a strong tailwind. In all three cases, the airplane would safely recover from the microburst encounter if the guidance algorithm were executed without human factors. The cases presented in Fig. 11 are examples of airplane crashes due to human factors when the pilot is represented by pilot

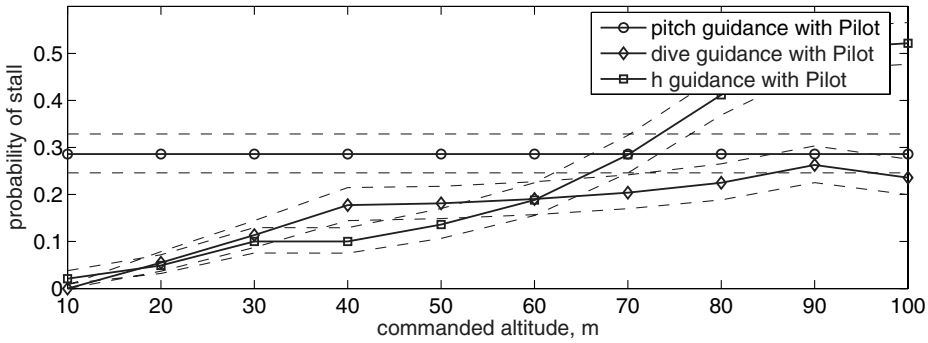

Fig. 12 Probability of stall with the three guidance strategies. 95% confidence limits are shown with thin dashed lines.

parameters at their corresponding expected values. It should be noted that the response trajectories can be significantly different depending on the microburst encountered, performance of the pilot, and the commanded altitude. Figure 12 shows the probability of the stall mode triggered with each guidance strategy. Note that as the commanded altitude increases, stall becomes more likely with altitude and dive guidance and even more so with altitude guidance for commanded altitudes higher than 70 m. When lower commanded altitude is used, the airplane trades altitude for airspeed and is exposed to smaller downdraft, that is, higher airspeed and less increase in angle of attack, and thus stall is less likely. However, when stall occurs at lower altitudes, it is more difficult for the pilot to safely execute the stall recovery maneuver because the airplane is too close to the ground. Although it is more likely to stall with higher commanded altitudes, the pilot may more safely recover from the stall because the airplane has enough altitude to trade for airspeed and for reducing the angle of attack. Further, as Fig. 4 implies, with the same commanded altitude, at the time of stall, the airplane will be at a higher altitude with dive guidance than with altitude guidance. Thus, even in the commanded altitude range in which dive and altitude guidance have about the same probability of stall, it will be more difficult for a pilot to recover from the stall when it occurs with the altitude guidance. This proposition is supported by the plot of the probability of recovering from a stall versus the commanded altitude. However, it does not give a statistically conclusive result because the confidence intervals are too large due to the fact that the number of simulation runs in which stall recovery maneuver is triggered is not large enough, and thus is not presented in this paper.

VII. Conclusions

A probabilistic approach has been used to study the effect of human factors on applications involving a wide variety of possible human operators. A case study analysis is conducted with specific application to recovering from a microburst using three different escape guidance strategies. A novel probabilistic approach is developed to model, instead of a single pilot, a group of pilots. Specific characteristic parameters that are representative of the personal attributes of the individual pilots are identified. These characteristic parameters are treated as random variables to model the variation among the individual pilots in terms of factors such as their skill, training, and experience. The Rayleigh PDF is chosen to be the probability density function for each of these parameters. The sensitivity of three escape guidance strategies, namely, pitch guidance, dive guidance, and altitude guidance to the human pilot factors were compared using a Monte Carlo simulation. In addition to the pilot's characteristic parameters, the strength, size, and location of the microburst were also treated as random variables. Although the strength of the microburst is varied according to the Rayleigh PDF, the size and location of the microburst are modeled as uniformly distributed random variables.

The simulation results indicate that dive guidance (with 40 m commanded altitude) gives the lowest probability of crash and the lowest probability of descending below 20 m. However, when considering minimum altitudes above 20 m, pitch guidance outperforms dive guidance. Further, pitch guidance is less sensitive to human factors than either dive guidance or altitude guidance. Thus, the pitch guidance is the most robust microburst escape guidance strategy in the sense that it is the least sensitive to human factors. This inference is in good agreement with the recommendation made by FAA's Windshear Training Aid. According to FAA, the other guidance strategies were considered to be worse compared to the pitch guidance strategy due to one/more of the following reasons.

1) The procedure does not provide as good a recovery profile as the recommended technique.

2) The procedure makes matters worse and in some cases may actually be dangerous.

3) The procedure complicates the recovery by increasing exposure to flight at an intermittent stick shaker.

The current study shows that when human factors are considered, the pitch and dive guidance strategies show the least dependence on the human pilot factors compared to the altitude guidance strategy. This is probably because of the fact that the pitch guidance procedure is simplest to execute, the dive guidance is slightly more complicated than the pitch guidance, and the altitude guidance is the most complicated strategy to implement. The only action to be taken by the pilot, as per the pitch guidance strategy, is to make the target pitch angle to be 15 deg as soon as the microburst is detected. In the case of dive guidance, the pilot's task is slightly more complicated as he needs to keep the pitch angle around 0 deg until the airplane descends to the commanded altitude and then he needs to pitch the airplane up to 15 deg. On the other hand, the altitude guidance strategy requires the pilot to fly the aircraft in different modes and switch from one mode to another while it is still under the effect of microburst windshear. Further, human factors cause the airplane to undershoot a commanded altitude and it is very hard for a pilot to bring the airplane back to the commanded altitude especially at low altitudes. Although the stall is less likely to occur when dive or altitude guidance with low commanded altitude is used, it is more difficult to recover because the airplane is too close to the ground; it is even more so with altitude guidance because altitude guidance attempts to keep the airplane at the commanded altitude while the dive guidance pitches the airplane to 15 deg to start increasing the altitude. Thus, altitude guidance strategy needs relatively greater effectiveness of pilot response in terms of reaction time, accurate stick movements, and better decision making. Therefore, altitude guidance strategy possesses higher sensitivity to the human factors than dive and especially pitch do.

The required next step of this work is that the probability density functions chosen for the various characteristic parameters of the human pilot be validated by obtaining relevant data from actual human pilots. Further, additional pilot parameters such as accuracy of following a control strategy can be included in Monte Carlo studies. The current study has shown that the probabilistic pilot modeling along with Monte Carlo simulation can provide valuable information in terms of the safety of a proposed strategy and more important its sensitivity to human factors. Furthermore, this approach can be used in different applications where the characteristics of the pilot are not deterministically predictable

or a group of pilots with statistically diverse characteristics are involved.

Acknowledgement

The authors would like to thank the Associate Editor and the anonymous reviewers for their constructive comments and suggestions that have improved the quality of the paper.

References

[1] Bengton, J., "Adaptive Cruise Control and Driver Modeling," Ph.D. Thesis, Lund Institute of Technology, Lund, Sweden, 2001.

[2] Arif, M., and Inooka, H., "Iterative Manual Control of Human Operator," *Biological Cybernetics*, Vol. 81, No. 5–6, May 1999, pp. 445–455.

[3] Enab, Y., "Controller Design for an Unknown Process, Using Simulation of a Human Operator," *Engineering Applications of Artificial Intelligence*, Vol. 8, No. 3, June 1995, pp. 299–308.

[4] McRuer, D., "Human Dynamics in Man-Machine Systems," *Automatica*, Vol. 16, No. 3, May 1980, pp. 237–253.

[5] McRuer, D., and Krendel, E., "The Human Operator as a Servo System Element," *Journal of the Franklin Institute*, Vol. 267, No. 6, June 1959, pp. 511–536.

[6] McRuer, D., and Ashkenas, I., "Design Implications of The Human Transfer Function," *IAS Man-Machine Competition Meeting*, IAS, 10–11 Aug. 1962.

[7] Kleinman, D., Baron, S., and Levison, W., "An Optimal Control Model of Human Response Part I: Theory and Validatio," *Automatica*, Vol. 6, No. 3, May 1970, pp. 357–369.

[8] Kleinman, D., and Baron, S., "A Control Theoretic Model for Piloted Approach to Landing," *Automatica*, Vol. 9, No. 3, May 1973, pp. 339–347.

[9] Magdaleno, R., McRuer, D., and Stapleford, R., "Pilot Describing Function Measurements in a Multiloop Task," NASA Center for AeroSpace Information (CASI), NASA CR-542, 19660801, 1 Aug. 1966.

[10] Hanley, J. G., "A Comparison of Nonlinear Algorithms to Prevent Pilot-Induced Oscillation Caused by Actuator Rate Limiting," Ph.D. Thesis, Air Force Institute of Technology, Ohio, May 2003.

[11] Ryu, S., "Longitudinal Flying Qualities and Controller Design for Nonlinear Aircraft," Ph.D. Thesis, Purdue University, Dec. 1999.

[12] David, J. M., "Human Piloting Factors in the Design of Control Laws for Precision Landing," Ph.D. Thesis, University of Dayton, Dayton, OH, Dec. 1993.

[13] Cacciabue, P., "A Methodology of Human Factors Analysis for Systems Engineering: Theory and Applications," *IEEE Transactions on Systems, Man and Cybernetics, Part A*, Vol. 27, May 1997, pp. 325–339.

[14] Rolfe, J., and Staples, K., *Flight Simulation*, Cambridge Univ. Press, Cambridge, U.K., 1986, pp. 209–230.

[15] McRuer, D., and Jex, H., "A Review of Quasi-Linear Pilot Models," *IEEE Transactions on Human Factor in Electronics*, Vol. 8, No. 3, Sept. 1967, pp. 231–249.

[16] Rodney, D. W., "An Evaluation of a Pilot Model Based on Kalman Filtering and Optimal Control," *IEEE Transactions on Man-Machine Systems*, Vol. 10, No. 4, Dec. 1969, pp. 108–117.

[17] Anderson, M., "A Model of the Human Operator Using Sensitivity Function Shaping," *Proceedings of the American Control Conference*, American Automatic Control Council, Green Valley, AZ, June 1994.

[18] Kaewchay, K., "Design of a Probabilistic Human Pilot: Application to Microburst Escape Maneuver," M.S. Thesis, University of Texas at Arlington, Arlington, TX, 2004.

[19] *Windshear Training Aid*, U.S. Department of Transportation, Federal Aviation Administration, Washington, D. C., 1987, pp. 4.4–287.

[20] Abdelrahman, M., Ghazi, M., Olwi, I., and Al-Bahi, A., "Aircraft Spoiler Effects Under Wind Shear," *Journal of Aircraft*, Vol. 31, No. 1, Jan.–Feb. 1994, pp. 154–160.

[21] Olwi, I., "Aerodynamic Characteristics of Aircraft Under Side Gust," *Journal of Aircraft*, Vol. 33, No. 5, Sept.–Oct. 1996, pp. 901–905.

[22] Maryniak, J., and Pedro, J., "Mathematical Modeling of the Effect of Windshear on the Dynamics of a Landing Aircraft," *Politechnika Slavaska, Zeszyty Naukowa, Mechanika*, Vol. 107, 1992, pp. 257–264 (in Polish).

[23] Ghazi, M., and Olwi, I., "Numerical Study of Windshear Effect on Fighter Aircraft During Power Approach," AIAA Paper 1995-3443, 1995.

[24] Bobbitt, R., and Howard, R., "Escape Strategies for Turboprop Aircarft in Microburst Windshear," *Journal of Aircraft*, Vol. 29, No. 5, Sept.–Oct. 1992, pp. 745–752.

[25] Miele, A., Wang, T., Melvin, W., and Bowles, R., "Maximum Survival Capability of an Aircraft in a Severe Wind Shear," *Journal of Optimization Theory and Applications*, Vol. 53, No. 2, May 1987, pp. 181–217.

[26] Mulgund, S., and Stengel, R., "Target Pitch Angle for the Microburst Escape Maneuver," *Journal of Aircraft*, Vol. 30, No. 6, Nov.–Dec. 1993, pp. 826–832.

[27] Mulgund, S., and Stengel, R., "Optimal Recovery from Microburst Wind Shear," *Journal of Guidance, Control, and Dynamics*, Vol. 16, No. 6, Nov.–Dec. 1993, pp. 1010–1017.

[28] Miele, A., Wang, T., and Melvin, W., "Optimization and Acceleration Guidance of Flight Trajectories in a Windshear," *Journal of Guidance, Control, and Dynamics*, Vol. 10, No. 4, July–Aug. 1987, pp. 368–377.

[29] Miele, A., "Optimal Trajectories and Guidance Trajectories for Aircraft Flight Through Windshears," *Proceedings of the 29th Conference on Decision and Control*, IEEE, Piscataway, NJ, Dec. 1990, CH2917-3.

[30] Zhao, Y., and Bryson, A., "Optimal Paths Through Downbursts," *Journal of Guidance, Control, and Dynamics*, Vol. 13, No. 5, 1990, pp. 813–818.

[31] Psiaki, M., and Stengel, R., "Optimal Aircraft Performance During Microburst Encounter," *Journal of Guidance, Control, and Dynamics*, Vol. 14, No. 2, 1991, pp. 440–446.

[32] Wang, H., "Optimization of Flight Trajectories in a 3D Model of Windshear Flow Field," Ph.D. Thesis, Rice University, Houston, TX, 1992.

[33] Visser, H., "Optimal Lateral Escape Maneuvers for Microburst Encounters During Final Approach," Delft Univ. of Technology, TR LR-691, Delft, The Netherlands, July 1992.

[34] Visser, H. G., "Optimal Lateral-Escape Maneuvers for Microburst Encounters During Final Approach," *Journal of Guidance, Control, and Dynamics*, Vol. 14, No. 6, Nov.–Dec., 1994, pp. 1234–1240.

[35] Visser, H., "Minimax Optimal Control Analysis of Lateral Escape Maneuvers for Microburst Encounters," *Journal of Guidance, Control, and Dynamics*, Vol. 20, No. 2, March–April 1997, pp. 370–376.

[36] Avila de Melo, D., "Analysis of Aircraft Performance During Lateral Maneuvering for Microburst Avoidance," M.S. Thesis, Department of Aeronautics and Astronautics, M.I.T., Cambridge, MA, 1989.

[37] Avila de Melo, D., and Hansman, R., "Analysis of Aircraft Performance During Lateral Maneuvering for Microburst Avoidance," *Journal of Aircraft*, Vol. 28, No. 12, 1991, pp. 837–842.

[38] Visser, H., "Lateral Escape Guidance Strategies for Microburst Windshear Encounters," *Journal of Aircraft*, Vol. 34, No. 4, July–Aug. 1997, pp. 514–521.

[39] Dogan, A., and Kabamba, P., "Escaping a Microburst with Turbulence: Altitude, Dive and Pitch Guidance Strategies," *Journal of Aircraft*, Vol. 37, No. 3, 2000, pp. 417–426.

[40] Dogan, A., and Kabamba, P., "Modified Guidance Laws to Escape Microbursts with Turbulence," *Mathematical Problems in Engineering*, Vol. 8, No. 1, 2002, pp. 43–67.

[41] Shank, E. M., and Hollister, K. M., "Precision Runway Monitor," *Lincoln Laboratory Journal*, Vol. 7, No. 2, 1994, pp. 329–354.

[42] Kuchar, J., "Methodology for Alerting-System Performance Evaluation," *Journal of Guidance, Control, and Dynamics*, Vol. 19, No. 2, 1996, pp. 438–444.

[43] Yang, L., and Kuchar, J., "Prototype Conflict Alerting System for Free Flight," *Journal of Guidance, Control, and Dynamics*, Vol. 20, No. 4, 1997, pp. 768–773.

[44] Hess, R., "Modeling the Effects of Display Quality upon Human Pilot Dynamics and Perceived Vehicle Handing Qualities," *IEEE Transaction On Systems, Man, Cybernetics*, Vol. 25, No. 2, Feb. 1995, pp. 338–344.

[45] Blakelock, J., *Automatic Control of Aircraft and Missiles*, 2nd ed., Wiley, New York, 1991, pp. 138–139.

[46] Vincent, B., and Pritchett, A., "Requirement Specification for Health Monitoring Systems Capable of Resolving Flight Control System Faults," *The 20th Conference Digital Avionics Systems, 2001, DASC*, IEEE, Piscataway, NJ, 14–18 Oct. 2001.

[47] Dogan, A., "Guidance Strategies for Microburst Escape," Ph.D. Thesis, University of Michigan, Ann Arbor, MI, 2000.

[48] Hosman, R., Benard, B., and Fourquet, H., "Active and Passive Side-Stick Controllers in Manual Aircraft Control," *Proceedings of IEEE International Conference on Systems, Man and Cybernetics*, IEEE, Piscataway, NJ, 4–7 Nov. 1990.

[49] Hess, R., "A Rational for Human Operator Pulsive Control Behavior," *Journal of Guidance, Control, and Dynamics*, Vol. 2, No. 3, May–June 1979, pp. 221–227.

[50] Metz, L. D., and Cyr, B., "Robust Control Performance of Time-Varying Human Controller Models," *Automatica*, Vol. 21, No. 4, July 1985, pp. 473–478.

[51] Stark, H., and Woods, J., *Probability, Random Process, and Estimation Theory for Engineering*, Prentice–Hall, Upper Saddle River, NJ, 1986, pp. 138–139.

[52] Sobol, I., *A Primer for the Monte Carlo Method*, CRC Press, Boca Raton, FL, 1994, pp. 35–59.

[53] Anderson, T. W., and Burstein, H., "Approximating the Upper Binomial Confidence Limit," *Journal of the American Statistical Association*, Vol. 62, No. 319, 1967, pp. 857–861.

[54] Anderson, T. W., and Burstein, H., "Approximating the Lower Binomial Confidence Limit," *Journal of the American Statistical Association*, Vol. 63, No. 324, 1967, pp. 1413–1415.